Sequential Determination of Kinematic Parameters in Assembled Parallel Kinematic Mechanisms

Bernhard Jokiel, Jr.
Sandia National Laboratories, Albuquerque, NM

John C. Ziegert
University of Florida Machine Tool Research Center, Gainesville, FL

1. Introduction

Over the last decade multi-axis machine tools and robots based on parallel kinematic mechanisms (PKMs) have been developed and marketed worldwide. Positional accuracy in these machines is controlled by accurate knowledge of the joint locations and distances between joint pairs (Figure 1.1). Since these machine tend to be rather large, the kinematic parameters are difficult to determine when these machines are in their fully assembled state. This work presents a method for determining the kinematic parameters of an assembled PKM where each kinematic parameter may be determined independently.

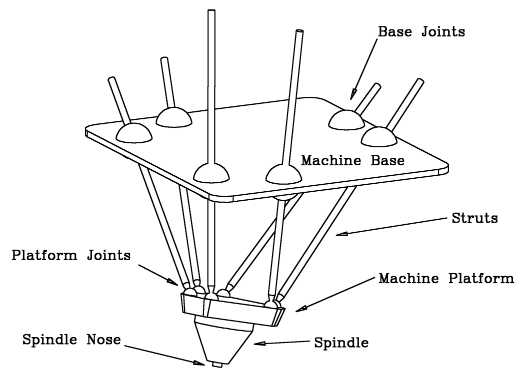

Figure 1.1: A 12-joint (6-6) Stewart platform six DOF device.

2. Sequential Determination Method

The proposed method has four parts: (1) locating a central reference frame, (2) identifying the joint center locations, (3) locating the spindle nose, and (4) determining the initial strut lengths.

2.1 Locating the Central Reference Frame (R)

Three gage points labelled r_1, r_2, and r_3 (usually some form of a kinematic mount) are secured at three corners of the worktable, creating a single fixed coordinate reference frame to which all future coordinate measurements collected in other floating reference frames will be transformed (Figure 2.1). Identifying the location of a chosen machine reference frame (M) may be performed at this time as well.

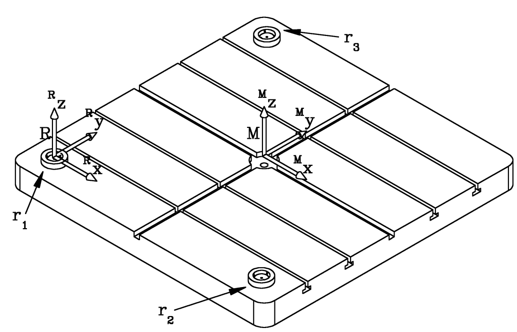

Figure 2.1: R and M reference frames.

2.2 Joint Center Location Identification

The platform is moved along an arbitrary predetermined path, while holding each strut in turn at an arbitrary fixed length. As the platform moves, the fixed-length strut rotates in its joints (Figures 2.2 and 2.3). Through measurement of the strut gage point coordinates and the corresponding platform poses, the locations of the base and platform joint centers may be determined by fitting the transformed gage point coordinates to the equation of a sphere. Assuming the joints produce spherical motion, the center of the calculated best-fit sphere is the center of rotation of the joint in question. Performing this method once for each of the six struts, the coordinates for all 12 of the base and platform joint centers may be recovered.

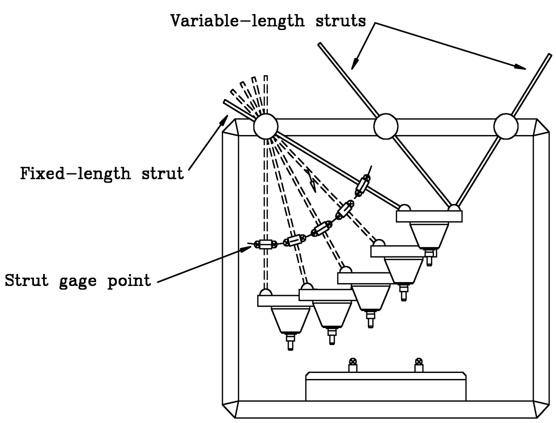

Figure 2.2: To an observer stationary relative to the M system, a point on the fixed length strut rotates about the base joint center.

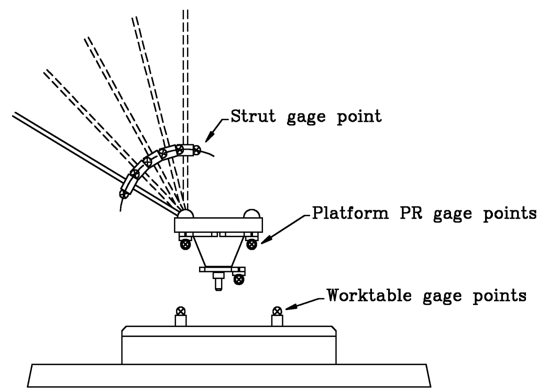

Figure 2.3: To an observer stationary relative to the PR system, a point on the fixed length strut rotates about the platform joint center.

2.3 Locating the Spindle Nose

A fixture holding a gage point attached to a tool holder mounted in the spindle is rotated slowly by hand. At approximately 30-40 different locations, the coordinates of the gage point are measured and fit to a skew circle (Figure 2.4). The unit normal vector of the best-fit plane is the unit orientation vector of the spindle relative to the PR system. The coordinates of the center of the circle projected along the positive direction of the normal vector by the offset distance are the coordinates of the center of the spindle nose.

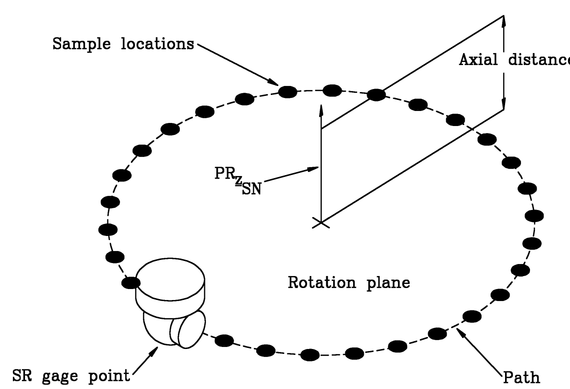

Figure 2.4: Spindle axis identification.

2.4 Determining the Initial Strut Lengths

The platform retracted to its home position. The coordinates of the PR gage points are measured. Knowing the locations of the base joints and the platform joints, the distances between the each of the six strut joint pairs are calculated. The platform is then moved from its home location, and the process is repeated. The initial strut reference length for each strut is taken to be the mean of the calculated strut lengths for each strut over all of the repetitions.

3. Uncertainty Analysis

The propagation of experimental data and machine positional uncertainties to the recovered kinematic parameters, and the propagation of the recovered parameter uncertainties to the tool tip were analyzed. The sequential determination method is dependent upon the accurate identification of the joint locations. To determine the uncertainty in the joint positions, it is necessary to quantify the amount of uncertainty present in the length of the struts.

3.1 Error Budget

Factors which influence the length of the strut between the fixture and the base joint (“Base”) are: joint motion sphericity, strut axial flexibility, thermal effects, strut length command mismatch, and the least count servo motion. Between the fixture and the platform joint (“Platform”) are: joint motion sphericity, strut axial flexibility, and thermal effects. Four distinct scenarios were considered (Table 3.1): (1) is the best estimate of the uncertainty present in the real system; (2) assumes measurements are perfect; (3) assumes the machine is perfect; and (4) is a more optimistic version of #1.

Table 3.1: Scenario input uncertainties.

Scenario	Base (mm)	Platform (mm)	Measurement (mm)
1	0.016	0.015	0.025
2	0.016	0.015	0.000
3	0.000	0.000	0.025
4	0.010	0.010	0.013

3.2 Uncertainty in Kinematic Parameters

Propagation of strut length and measurement uncertainties to the recovered kinematic parameters was done by a Monte Carlo simulation. Each scenario was subjected to 10000 iterations. First, the reverse kinematic solver calculated the nominal strut lengths for the pose in each particular fixed-length strut toolpath given the set of nominal kinematic parameters. For each iteration, a small amount of uniformly distributed, random strut length uncertainty was added to the strut lengths. The new pose of the platform and gage point locations were calculated. Uniformly distributed, random measurement uncertainty was added to the gage point locations. Finally, the joint center locations and initial strut lengths were determined from the perturbed gage point locations. The mean and standard deviation of the sphericity and the center error distance (CED) were also calculated over all of the iterations for each scenario. Table 3.2 shows the results for strut 1, which are representative of the results for the other 5 struts.

Table 3.2: Joint center uncertainty.

	Scenario Number	Base Joint Mean (mm)	Base Joint σ (mm)	Platform Joint Mean (mm)	Platform Joint σ (mm)
Sphericity	1	0.045	0.008	0.064	0.014
	2	0.029	0.004	0.027	0.003
	3	0.033	0.006	0.057	0.013
	4	0.026	0.005	0.035	0.007
CED	1	0.067	0.044	0.098	0.064
	2	0.048	0.031	0.045	0.028
	3	0.050	0.032	0.086	0.057
	4	0.039	0.025	0.054	0.035

In a similar manner the propagation of the machine and measurement uncertainties to the initial strut lengths were calculated (Table 3.3).

Table 3.3: Uncertainty in the initial strut lengths.

Scenario	$\sigma_{Strut\ 1}$ (mm)	$\sigma_{Strut\ 2}$ (mm)	$\sigma_{Strut\ 3}$ (mm)	$\sigma_{Strut\ 4}$ (mm)	$\sigma_{Strut\ 5}$ (mm)	$\sigma_{Strut\ 6}$ (mm)
1	0.139	0.162	0.122	0.134	0.287	0.160
2	0.066	0.071	0.060	0.067	0.123	0.076
3	0.123	0.147	0.106	0.118	0.257	0.141
4	0.077	0.089	0.067	0.075	0.157	0.088

3.3 Uncertainty in Machine Motion

A Monte Carlo simulation was used to propagate the uncertainties in the calibration to the tool tip. First, path plans for six circular traces were developed (Table 3.4). Second, the inverse kinematics calculated the nominal poses of the mechanism for each path from the nominal parameters. Third, 1000 sets of parameters were selected from the 10000 previously simulated.

For each set, scenario and pose in each circular path, the error between the nominal and the recovered simulated parameters were calculated and projected on to the strut lines of action. Additional uniformly, randomly distributed strut length uncertainties were added. The forward kinematics determined the perturbed tool tip locations for each path. Using the perturbed tool tip locations the best-fit circle was calculated for each path.

Table 3.4: Locations of circular traces.

Circle Number	Nominal Circle Locations (mm) X	Y	Z	Radius
1	0	0	180	150
2	200	200	180	150
3	-200	200	180	150
4	-200	-200	180	150
5	200	-200	180	150
6	0	0	180	300

For each circular trace and uncertainty scenario, the mean and standard deviation of the X and Y circle center coordinates, radii and circularities were calculated over all of the iterations. Results for circle #1 for all four scenarios is shown in Table 3.5 and are representative of the other five traces.

Table 3.5: Circle #1 location uncertainty.

Scenario	$\overline{X}$ (mm)	σ_X (mm)	$\overline{Y}$ (mm)	σ_Y (mm)	$\overline{R}$ (mm)	σ_R (mm)	$\overline{Circ.}$ (mm)	σ_{Circ} (mm)
1	0.000	0.038	0.001	0.038	150.000	0.002	0.115	0.008
2	-0.001	0.018	0.000	0.018	150.000	0.001	0.115	0.008
3	0.001	0.033	-0.001	0.032	150.000	0.001	0.003	0.002
4	-0.001	0.021	0.000	0.021	150.000	0.001	0.074	0.005

4. Experimental Results

A total of three complete and independent trials were run of the proposed sequential determination method on a Hexel milling machine installed at Sandia National Laboratories. A SMX 4000 laser tracker was used to collect the spatial coordinate data for the kinematic parameter recovery. Fro brevity, the results for the kinematic parameters for each trial will not be listed here. However, interested readers are encouraged to contact the authors who will provide complete results.

Each of the three new kinematic parameter databases, as well as the original, were loaded into the machine controller. The machine was then commanded to follow the six circular traces listed in Table 3.4. The circular traces were measured using a Renishaw ball bar. Results appear in Table 4.1.

Table 4.1: Renishaw ball bar circular trace results.

Database	Circle Number	Radial Deviation Max µm	Min µm	Best-Fit Radius mm	Center Position X µm	Y µm
Original	1	32.2	-30.6	149.987	-7.2	-37.2
	2	27.5	-26.1	150.010	-32.6	-41.2
	3	61.1	-71.2	149.996	14.4	-21.1
	4	42.9	-37.1	149.965	-11.5	-5.5
	5	57.1	-56.2	149.987	-34.9	-21.1
	6	68.8	-61.3	299.996	1.0	-15.1
Trial 1	1	20.3	-20.1	149.978	-17.8	-39.9
	2	20.0	-27.1	149.990	-21.3	-25.9
	3	33.3	-40.5	149.986	3.7	-21.8
	4	45.5	-41.0	149.961	-18.1	-20.1
	5	46.5	-43.4	149.977	-10.9	-14.8
	6	41.3	-41.0	299.973	18.8	-9.5
Trial 2	1	24.6	-26.6	149.998	-36.9	-26.6
	2	36.5	-42.0	149.994	-50.9	-15.0
	3	46.6	-50.6	150.005	-5.0	-11.8
	4	35.8	-30.5	149.995	-6.5	4.8
	5	46.9	-35.9	149.994	-9.3	6.4
	6	59.0	-61.2	300.007	-8.7	-17.7
Trial 3	1	27.2	-31.6	149.996	13.8	-24.5
	2	22.6	-29.1	150.012	-14.4	-14.5
	3	19.5	-24.6	150.003	18.0	-16.6
	4	53.2	-63.3	149.982	-13.6	-23.2
	5	52.9	-56.9	150.003	-11.1	-0.9
	6	48.6	-56.5	300.022	18.1	-27.5

5. Conclusions

The theoretical and experimental evaluation of the proposed sequential determination method for identifying the kinematic parameters in fully assembled Stewart platform type PKMs appears to show that it is a viable technique.

Monte Carlo simulations show measurement uncertainty appears to have the greatest impact on the correct identification of the joint centers and the initial strut lengths. Uncertainties in the machine strut lengths does not appear to have as great of an effect on the recovered parameters.

The Renishaw ball bar circles used to evaluate the success of the calibration appear to show that the correct kinematic parameters were identified, although a great improvement in machine performance did not appear to have occurred. However, a rigorous application of the ASME B5.54 standard is warranted to decisively show improvements in positional accuracy.

References

[1] Jokiel, Jr. Bernhard. "Sequential Determination of Kinematic Parameters in Assembled Parallel Kinematic Mechanisms." Ph.D. Dissertation, University of Florida, 1999.

[2] Wang, Jian and Oren Masory. "On the Accuracy of a Stewart Platform - Part I The Effect of Manufacturing Tolerances." Proceedings IEEE International Conference on Robotics and Automation, Vol. 1, 1993. Los Alamitos, California: IEEE Computer Society Press, pages 114-120.

[3] Masory, Oren, Jian Wang, and Hanqi Zhuang. "On the Accuracy of a Stewart Platform - Part II Kinematic Calibration and Compensation." Proceedings IEEE International Conference on Robotics and Automation, Vol. 1, 1993. Los Alamitos, California: IEEE Computer Society Press, pages 725-731.

[4] Zhuang, Hanqi and Zvi S. Roth. "Method for Kinematic Calibration of Stewart Platforms." Journal of Robotic Systems, Vol. 10, No. 3, 1993. pages 391-405

[5] Zhuang, Hanqi. Lixin Liu and Oren Masory. "Autonomous Calibration of Hexapod Machine Tools." ASME Journal of Manufacturing Science and Technology, Vol 19, 1997. pages 202-211.

[6] Bourdet, P., C. Lartigue, and F. Leveaux. "Effects of Data Point Distribution and Mathematical Model on Finding the Best-Fit Sphere to Data." Precision Engineering. Vol. 15 No. 3, 1993. pages 150-157.

[7] Taylor, Barry N., Chris E. Kuyatt. "Guidelines for Evaluating and Expressing the Uncertainty of NIST Measurement Results." National Institute of Standards and Technology, NIST Technical Note 1297, 1994.